

Article

# On the Wavelet Collocation Method for Solving Fractional Fredholm Integro-Differential Equations

Haifa Bin Jebreen <sup>1,\*</sup>  and Ioannis Dassios <sup>2,†</sup> 

<sup>1</sup> Department of Mathematics, College of Science, King Saud University, P.O. Box 2455, Riyadh 11451, Saudi Arabia

<sup>2</sup> AMPSAS, University College Dublin, D04 V1W8 Dublin, Ireland; ioannis.dassios@ucd.ie

\* Correspondence: hjebreen@ksu.edu.sa

† These authors contributed equally to this work.

**Abstract:** An efficient algorithm is proposed to find an approximate solution via the wavelet collocation method for the fractional Fredholm integro-differential equations (FFIDEs). To do this, we reduce the desired equation to an equivalent linear or nonlinear weakly singular Volterra–Fredholm integral equation. In order to solve this integral equation, after a brief introduction of Müntz–Legendre wavelets, and representing the fractional integral operator as a matrix, we apply the wavelet collocation method to obtain a system of nonlinear or linear algebraic equations. An a posteriori error estimate for the method is investigated. The numerical results confirm our theoretical analysis, and comparing the method with existing ones demonstrates its ability and accuracy.

**Keywords:** wavelet collocation method; fractional integro-differential equation; Müntz–Legendre wavelets

**MSC:** 65L60; 47G20; 65T60



**Citation:** Bin Jebreen, H.; Dassios, I. On the Wavelet Collocation Method for Solving Fractional Fredholm Integro-Differential Equations. *Mathematics* **2022**, *10*, 1272. <https://doi.org/10.3390/math10081272>

Academic Editor: Nickolai Kosmatov

Received: 22 March 2022

Accepted: 7 April 2022

Published: 12 April 2022

**Publisher's Note:** MDPI stays neutral with regard to jurisdictional claims in published maps and institutional affiliations.



**Copyright:** © 2022 by the authors. Licensee MDPI, Basel, Switzerland. This article is an open access article distributed under the terms and conditions of the Creative Commons Attribution (CC BY) license (<https://creativecommons.org/licenses/by/4.0/>).

## 1. Introduction

In this study, we propose an efficient scheme for solving the fractional Fredholm integro-differential equations (FFIDEs) of order  $\alpha$  ( $\alpha \in \mathbb{R}^+$ ) on the finite interval  $[0, 1]$

$${}^C\mathcal{D}_0^\alpha y(x) = c_1 f(x, y(x)) + c_2 \int_0^1 k(x, t)g(y(t))dt, \quad x \in [0, 1], \quad (1)$$

with the Caputo fractional derivative  ${}^C\mathcal{D}_0^\alpha$  and initial conditions

$$y^\nu(0) = y_\nu, \quad \nu = 0, \dots, n-1, \quad (2)$$

in which  $c_1, c_2$  are constants,  $[\alpha] + 1 := n \in \mathbb{N}$ , for  $\alpha \notin \mathbb{N}$  and  $n = \alpha$  for  $\alpha \in \mathbb{N}$ . Here, the function  $f$  is assumed to be a sufficiently smooth linear or nonlinear function on  $\Omega \times \mathbb{R}$  with  $\Omega := [0, 1]$ ,  $k$  is a continuous function on  $\Omega^2 := \Omega \times \Omega$ , and the linear or nonlinear function  $g$  is assumed to be continuous and satisfies the Lipschitz condition

$$|g(y) - g(v)| \leq \rho |y - v|, \quad (3)$$

where  $\rho > 0$  is the Lipschitz constant.

These types of equations have a very valuable role in modeling some physical phenomena, such as glass-forming process [1], epidemic processes [2], and viscoelasticity [3]. There exist several papers that offer analytical methods for solving such equations. However, when the problem is complicated, the existing analytical methods no longer work and we cannot find the exact solution. Therefore, numerical methods are often suggested to solve this problem. In [4], the Spline collocation method is applied to solve the problem.

Momani et al. [5,6] used the Adomian decomposition method for solving the fourth-order and systems of FFIDEs. To solve a special type of these equations, i.e.,

$${}^C\mathcal{D}_0^\alpha y(x) - \lambda \int_0^1 k(x,t)[y(t)]^v dt = f(x), \quad v > 1, \tag{4}$$

with the initial conditions

$$y^{(i)}(0) = \delta_i, \quad i = 0, \dots, n-1, \quad n-1 < \alpha \leq n,$$

Zhu et al. [7] proposed the Galerkin method based on the Chebyshev wavelet. After introducing the Chebyshev wavelet and the operational matrix of the Riemann–Liouville fractional integral for this basis, they used the Galerkin method to reduce (4) to a system of algebraic equations. The fractional differential transform scheme is used to solve the equation [8]. Saeedi et al. [9] used the same procedure based on CAS wavelets. Shahmorad et al. [10] proposed the Tau-like numerical algorithm to solve the delay fractional integro-differential equation. To read more about the methods provided, please refer to [11,12].

Recently, the Müntz–Legendre wavelets have been applied to find the numerical solution of some equations, such as fractional pantograph differential equations [13], fractional optimal control problems [14], fractional differential equations [15] and multi-order fractional differential equations [16].

The outline of this article is as follows: In Section 2, we provide an introduction to fractional calculation and introduce the Müntz–Legendre wavelets. Section 3 is dedicated to the application of the wavelet collocation method for solving FFIDEs. In this section, an a posteriori error estimate is also surveyed. In Section 4, some numerical implementations are performed to demonstrate the accuracy and efficiency of the method.

## 2. Preliminaries

We begin this section with a brief introduction to fractional calculus and the Müntz–Legendre wavelets (ML wavelets).

### 2.1. Fractional Calculation

**Definition 1.** Let  $\alpha \in \mathbb{R}^+$ , we specify the Riemann–Liouville (RL) fractional integral operator  $\mathcal{I}_a^\alpha$  via

$$\mathcal{I}_a^\alpha(f)(x) := \frac{1}{\Gamma(\alpha)} \int_a^x (x - \zeta)^{\alpha-1} f(\zeta) d\zeta, \quad x \in [a, b], \quad f \in L_1[a, b], \tag{5}$$

in which  $\Gamma(\alpha)$  is the Gamma function.

With this definition, it is easy to verify that

$$\mathcal{I}_a^\alpha(x^\beta) = \frac{\Gamma(\beta + 1)}{\Gamma(\beta + \alpha + 1)} x^{\beta+\alpha}. \tag{6}$$

**Lemma 1** (cf. Lemma 2.1 (a), [17]). Given  $1 \leq p \leq \infty$ , the operator  $\mathcal{I}_a^\alpha$  is bounded in  $L^p([a, b])$ , i.e.,

$$\|\mathcal{I}_a^\alpha(f)\|_p \leq \frac{(b-a)^\alpha}{\Gamma(\alpha + 1)} \|f\|_p. \tag{7}$$

**Definition 2.** The Riemann–Liouville operator of fractional derivative is defined by

$${}^R\mathcal{D}_a^\alpha(f)(x) := \mathcal{D}^n \mathcal{I}_a^{n-\alpha}(f)(x) = \frac{1}{\Gamma(n-\alpha)} \mathcal{D}^n \int_a^x (x-t)^{n-\alpha-1} f(t) dt, \tag{8}$$

where  $\alpha \in \mathbb{R}^+$ ,  $[\alpha] + 1 := n \in \mathbb{N}$  and  $\mathcal{D}^n := \frac{d^n}{dx^n}$ .

There exists another fractional derivative operator that can replace the Riemann–Liouville fractional derivative.

**Definition 3.** The Caputo fractional derivative is determined by [17].

$${}^c\mathcal{D}_a^\alpha(f)(x) := \frac{1}{\Gamma(n-\alpha)} \int_a^x \frac{f^{(n)}(\zeta)d\zeta}{(x-\zeta)^{\alpha-n+1}} =: \mathcal{I}_a^{n-\alpha}\mathcal{D}^n(f)(x), \tag{9}$$

in which  $\alpha \in \mathbb{R}^+$  and  $[\alpha] + 1 := n \in \mathbb{N}$ .

**Lemma 2** (cf. Corollary 2.3 (a), [17]). It can be proved that the Caputo fractional derivative operator  ${}^c\mathcal{D}_a^\alpha$  is bounded via

$$\|{}^c\mathcal{D}_a^\alpha(f)\|_C \leq \frac{1}{\Gamma(n-\alpha)(n-\alpha+1)} \|f\|_{C^n}, \tag{10}$$

where  $\alpha \in \mathbb{R}^+$ ,  $\alpha \notin \mathbb{N}_0$  and  $n = -[-\alpha]$ .

### 2.2. Müntz–Legendre Wavelets

For  $J \in \mathbb{N}_0$  and  $r \in \mathbb{N}$ , let  $\mathcal{R} := \{0, 1, \dots, r-1\}$  and  $\mathcal{B} := \{0, 1, \dots, 2^J - 1\}$ . Then assume that the sub-space  $A_J \in L^2(\Lambda)$  is spanned by

$$A_J = \text{span}\{\phi_{J,b}^n : n \in \mathcal{R}, b \in \mathcal{B}\},$$

in which  $\phi_{J,b}^n$  is the scaled and translated version of  $\phi^n$ , and  $\Lambda$  is a bounded interval or  $\Lambda := \mathbb{R}$ . Furthermore, the parameters  $J$  and  $r$  are called the refinement level and multiplicity, respectively.

At the sequel, we give a brief introduction to the ML wavelets that, in addition to spanned  $V_J$ , they also satisfy certain circumstances [18] (namely, multiresolution analysis (MRA)).

Motivated by [19], an increasing sequence  $\mathcal{L} = \{0 = \lambda_0 < \lambda_1 < \dots\}$  guarantees that the vector space

$$P(\mathcal{L}) := \bigcup_{n=0}^{\infty} P_n(\mathcal{L}) = \text{span}\{x^{\lambda_n}, n = 0, 1, \dots\}, \quad x \in (0, 1),$$

spanned by  $\{x^{\lambda_n}\}_{n=0}^{\infty}$  and is a dense subset of  $C[0, 1]$ . Here  $P_n(\mathcal{L}) := \text{span}\{x^{\lambda_0}, x^{\lambda_1}, \dots, x^{\lambda_n}\}$  for each  $n$ . The Russian mathematician S. N. Bernstein specifically proved that the sufficient and necessary conditions to have  $\overline{P(\mathcal{L})} = C[0, 1]$  are

$$\sum_{\lambda_k > 0} \frac{1 + \log \lambda_k}{\lambda_k} = \infty,$$

and

$$\lim_{k \rightarrow \infty} \frac{\lambda_k}{k \log k} = 0,$$

respectively. He also conjectured that the necessary and sufficient condition to have  $\mathcal{L} = \{0 = \lambda_0 < \lambda_1 < \dots\}$  is

$$\sum_{k=1}^{\infty} \frac{1}{\lambda_k} = \infty.$$

Two years later, Müntz proved this conjecture [20]. It can be shown that the same result can be held for  $L^2(0, 1)$  [21]. It is worth noting that the functions  $\{x^{\lambda_n}\}_{n=0}^{\infty}$  are not suitable as basis functions. Thus, in the sequel, the Müntz–Legendre functions will be introduced such that they are easy to evaluate and are orthogonal.

Motivated by [21,22], the ML polynomials are determined by

$$L_n(x; \mathcal{L}) := \frac{1}{2\pi i} \int_A \prod_{k=1}^{n-1} \frac{s + \lambda_k + 1}{s - \lambda_k} \frac{x^s}{s - \lambda_n} ds, \tag{11}$$

where  $A$  is a simple contour which is circumambient to all zeros of the denominator in the integrand. The aforementioned polynomials can be shown via

$$L_n(x; \mathcal{L}) = \sum_{l=0}^n l_{l,n} x^{\lambda_l}, \quad x \in [0, 1], \tag{12}$$

where the coefficient  $l_{l,n}$  is obtained by

$$l_{l,n} := \frac{\prod_{i=0}^{n-1} (\lambda_l + \lambda_i + 1)}{\prod_{i=0, i \neq l}^n (\lambda_l - \lambda_i)}. \tag{13}$$

in which  $\lambda_l := \{l\mu : \mu \in \mathbb{R}, l = 0, \dots, n\}$ . It can easily be shown that the ML polynomials are orthogonal [21,22].

For simplicity, assume that  $L_n(x) := L_n(x; \mathcal{L})$  from now on. According to the definition of  $L_n(x)$ , the ML wavelets [16] can be obtained via

$$\phi_{J,b}^n = \begin{cases} 2^{J/2} \sqrt{2\lambda_n + 1} L_n(2^J x - b), & \frac{b}{2^J} \leq x \leq \frac{b+1}{2^J}, \\ 0, & \text{otherwise.} \end{cases} \tag{14}$$

Motivated by ML wavelets, we introduce a projection operator  $\mathcal{P}_J$  that maps any function  $y \in L^2([0, 1])$  onto  $A_J$  as follows.

$$y(x) \approx \mathcal{P}_J(y)(x) = \sum_{b=0}^{2^J-1} \sum_{n=0}^{r-1} y_{b,n} \phi_{J,b}^n(x) = U^T \Phi(x) \in A_J, \tag{15}$$

where  $\Phi(x)$  is a  $N = 2^J r$  dimensional vector function whose  $(br + n + 1)$ -th element is  $\phi_{J,b}^n(x)$ . To evaluate the element of vector  $U$ , we have

$$y_{b,n} = \langle y, \phi_{J,b}^n \rangle = \int_0^1 y(x) \phi_{J,b}^n(x) dx. \tag{16}$$

The aforementioned expansion (15) can be bounded as follows [13].

**Lemma 3 ([13]).** *If  $y \in H^m([0, 1])$  for  $r > m$ , then*

$$\|y - \mathcal{P}_J(y)\|_{L_2([0,1])} \leq c(r - 1)^{-m} (2^{J-1})^{-m} \|y^{(m)}\|_{L_2([0,1])}, \tag{17}$$

and when  $s \geq 1$ , we get

$$\|y - \mathcal{P}_J(y)\|_{H^s([0,1])} \leq c(2^{J-1})^{s-m} (r - 1)^{2s-\frac{1}{2}-m} \|y^{(m)}\|_{L_2([0,1])}, \tag{18}$$

in which  $H^m([0, 1])$  is the Sobolev space and the related norm is determined by

$$\|y\|_{H^m([0,1])} = \left( \sum_{j=0}^m \|y^{(j)}\|_{L_2([0,1])}^2 \right)^{1/2}.$$

### 2.3. Representation of Fractional Integral Operator in ML Wavelets

The fractional integration of the vector function  $\Phi_J(x)$  can be expressed by

$$\mathcal{P}_J(\mathcal{I}_0^\alpha)(\Phi(x)) \approx I_\alpha \Phi(x), \quad x \in (0, 1), \tag{19}$$

where  $I_\alpha$  is called the Riemann–Liouville fractional operational matrix.

In order to find the elements of  $I_\alpha$  for ML wavelets, we need to introduce the piecewise fractional-order Taylor functions, i.e.,

$$\psi_{j,b}^n = \begin{cases} t^{\lambda_n}, & \frac{b}{2^j} \leq x \leq \frac{b+1}{2^j}, \\ 0, & \text{otherwise,} \end{cases} \quad b \in \mathcal{B}, n \in \mathcal{R}, j \in \mathbb{Z}^+ \cup \{0\}. \tag{20}$$

Using the vector function  $\Psi(x)$  whose elements are  $\psi_{j,b}^n$ , the vector function  $\Phi(x)$  (ML wavelets) can be represented by

$$\Phi(x) = T^{-1}\Psi(x), \tag{21}$$

where the transformation matrix  $T$  is the square matrix of dimension  $N \times N$  with elements

$$T_{i,j} = \langle \Phi_i(x), \Psi_j(x) \rangle = \int_0^1 \Phi_i(x)\Psi_j(x)dx, \quad i, j = 1, \dots, N. \tag{22}$$

It can be shown that

$$\Psi(x) = [V, \dots, V]^T, \tag{23}$$

in which  $V$  is assumed to be a  $r$ -dimension vector whose  $i$ -th element is  $x^{\lambda_i}$ . From (6), one can calculate the fractional integral of the  $i$ -th element  $\Psi(x)$ , i.e.,

$$\mathcal{I}_0^\alpha(\Psi_i)(x) = \frac{\Gamma(\lambda_i + 1)}{\Gamma(\lambda_i + \alpha + 1)} x^{\lambda_i + \alpha}. \tag{24}$$

Therefore, there exists a matrix  $I_{\Psi,\alpha}(x)$  such that

$$\mathcal{I}_0^\alpha(\Psi)(x) = I_{\Psi,\alpha}(x)\Psi(x). \tag{25}$$

It can easily be demonstrated that

$$I_{\Psi,\alpha}(x) = \text{diag}[P_\alpha(x), \dots, P_\alpha(x)],$$

in which  $P_\alpha(x) := x^\alpha Q (\mathcal{I}_0^\alpha(V)(x) = P_\alpha(x)V(x))$ , and  $Q$  is a diagonal matrix

$$(Q)_{i,i} = (\Gamma(\lambda_i + 1))(\Gamma(\lambda_i + \alpha + 1))^{-1}.$$

Now, we can obtain the fractional integral operational matrix for the ML wavelets

$$\begin{aligned} \mathcal{P}_J(\mathcal{I}_0^\alpha)(\Phi(x)) &= \mathcal{P}_J(\mathcal{I}_0^\alpha)(T^{-1}\Psi(x)) \\ &= T^{-1}I_{\Psi,\alpha}(x)\Psi(x) \\ &= T^{-1}I_{\Psi,\alpha}(x)T\Phi(x). \end{aligned}$$

Thus we obtain

$$I_\alpha(x) := T^{-1}I_{\Psi,\alpha}(x)T. \tag{26}$$

### 3. Wavelet Collocation Method

In the present section, we utilize the collocation method based on ML wavelets to obtain an approximate solution of the fractional Fredholm integro-differential Equation (1). In the operator form, Equation (1) may be written as

$$({}^C\mathcal{D}_0^\alpha - c_2\mathcal{K})y = c_1f, \tag{27}$$

in which the operator  $\mathcal{K}$  is denoted by

$$\mathcal{K}(y)(x) := \int_0^1 k(x,t)g(y(t))dt. \tag{28}$$

If  $y$  is a sufficiently smooth function on  $[0, 1]$ , it can be proved that Equation (1) has a unique solution  $y(x)$  on  $[0, 1]$ .

**Lemma 4.** Given  $\alpha \in \mathbb{R}^+$ , let  $n = -[-\alpha]$ . Assume that  $f, k$ , and  $u$  are continuous functions. Then  $y(x)$  is the solution of (1) if, and only if,  $y(x)$  satisfies the integral equation

$$y(x) = \sum_{j=0}^{n-1} \frac{y^{(j)}(0)}{j!} x^j + c_1 \mathcal{I}_0^\alpha(f)(x, y(x)) + c_2 \mathcal{I}_0^\alpha \mathcal{K}(y)(x), \tag{29}$$

**Proof.** The proof is similar to the proof of Theorem 3.24 in [17].  $\square$

To obtain the discretization of (29), the numerical solution may be approximated by the operator  $\mathcal{P}_J$ , i.e.,

$$y(x) \approx \mathcal{P}_J(y)(x) = U^T \Phi(x) := y_J(x), \tag{30}$$

where  $U$  is a  $N$ -dimension vector whose elements should be found. Replacing (30) into (29), we get

$$y_J(x) = \sum_{j=0}^{n-1} \frac{y^{(j)}(0)}{j!} x^j + c_1 \mathcal{I}_0^\alpha(f)(x, y_J(x)) + c_2 \mathcal{I}_0^\alpha(\mathcal{K})(y_J)(x). \tag{31}$$

Now, we transfer all terms in (31) onto  $A_J$  via the projection operator  $\mathcal{P}_J$  as follows

- Let us put  $p_1(x) := \sum_{j=0}^{n-1} \frac{y^{(j)}(0)}{j!} x^j$ , then we can write

$$p_1(x) \approx \mathcal{P}_J(p_1)(x) = P_1^T \Phi(x), \tag{32}$$

where the  $j$ -th element of the  $N$  dimensional vector  $P_1$  is obtained by  $\langle p_1, \Phi_j \rangle$ .

- After putting the approximate solution  $y_J$  into  $g(y(t))$  and then approximating it and the kernel function  $k(x, t)$  using operator  $\mathcal{P}_J$ , we have

$$\begin{aligned} p_2(t) &:= g(y_J(t)) \approx \mathcal{P}_J(g(y_J(t))) = G^T \Phi(t), \\ k(x, t) &\approx \mathcal{P}_J(k)(x, t) = \Phi^T(x) K \Phi(t), \end{aligned} \tag{33}$$

where  $G$  is an  $N$ -dimensional vector whose  $j$ -th element is  $\langle p_2, \Phi_j \rangle$ , and  $K$  is a square matrix of dimension  $N \times N$  whose  $(i, j)$ -element is

$$K_{i,j} = \int_0^1 \int_0^1 k(x,t) \Phi_i(x) \Phi_j(t) dx dt.$$

Replacing (33) into  $\mathcal{K}(y_J)(x)$ , we obtain

$$\mathcal{P}_J \mathcal{K}(y_J)(x) \approx G^T K^T \Phi(x) \in A_J, \tag{34}$$

To give rise to the discretized form of  $\mathcal{I}_0^\alpha \mathcal{K}(y_J)(x)$ , using the operational matrix  $I_\alpha$  and (35), we obtain

$$\mathcal{I}_0^\alpha \mathcal{K}(y_J)(x) \approx G^T K^T I_\alpha(x) \Phi(x). \tag{35}$$

- In the same way as the previous item, we can use the projection  $\mathcal{P}_J$  for the term  $\mathcal{I}_0^\alpha(f)(s, y(s))$ , as

$$\begin{aligned} \mathcal{I}_0^\alpha(f)(s, y_J(s)) &\approx \mathcal{I}_0^\alpha(F^T \Phi(x)) \\ &\approx F^T I_\alpha(x) \Phi(x), \end{aligned} \tag{36}$$

where  $F$  is a  $N$ -dimension vector whose  $j$ -th element is  $\langle f, \Phi_j \rangle$ .

Now we refer to (29) and rewrite it using (32), (35) and (36) as follows.

$$r(x) := \left( U^T - P_1^T - c_1 F^T I_\alpha(x) - G^T K^T I_\alpha(x) \right) \Phi(x) = 0, \tag{37}$$

where  $r(x)$  is the residual function that our goal is to reduce to zero. By choosing the collocation points  $\{x_i\} \in \Omega$  which satisfy  $r(x_i) = 0$ , we obtain a system of nonlinear or linear algebraic equations. After solving this system, we can find the unknown coefficients  $U$ . Here, the collocation points are chosen so that they are the roots of the shifted Chebyshev and Legendre polynomials.

*Error Analysis*

**Theorem 1.** Assume that  $k(x, t)$  is a sufficiently smooth function on  $[0, 1] \times \mathbb{R}$  and the functions  $g$  and  $f$  are continuous and satisfy the Lipschitz conditions (3) and

$$|f(x, y(x)) - f(x, v(x))| \leq \varrho |y - v|, \tag{38}$$

respectively.

If  $c_1 \frac{\rho M_1}{\alpha \Gamma(\alpha)} + c_2 \frac{\varrho}{\Gamma(\alpha+1)} < 1$  with  $\alpha \in (0, 1)$ , and  $M_1 = \max_{x,t \in [0,1]} |k(x, t)|$ , then the a posteriori error estimate can be found as,

$$\|y(x) - y_J(x)\| \leq \frac{C}{1 - \eta} (r - 1)^{-m} (2^{J-1})^{-m}.$$

**Proof.** Motivated by Lemma 3, we have

$$\|\mathcal{I}_0^\alpha \mathcal{K}(y_J) - \mathcal{P}_J \mathcal{I}_0^\alpha \mathcal{K}(y_J)\| \leq c_0 (r - 1)^{-m} (2^{J-1})^{-m} M_2, \tag{39}$$

where  $M_2 = \max\{\mathcal{D}^m \mathcal{I}_0^\alpha \mathcal{K}(y_J)\}$ , and to approximate it, we can consider two situations.

1. if  $m < n$ , then we have

$$\mathcal{D}^m \mathcal{I}_0^\alpha \mathcal{K}(y_J) = \mathcal{I}_0^{\alpha-m} \mathcal{K}(y_J), \tag{40}$$

and it follows from Lemma 1 that

$$\begin{aligned} \|\mathcal{D}^m \mathcal{I}_0^\alpha \mathcal{K}(y_J)\| &= \|\mathcal{I}_0^{\alpha-m} \mathcal{K}(y_J)\| \leq \frac{1}{\Gamma(\alpha - m + 1)} \|\mathcal{K}(y_J)\| \\ &\leq \frac{M_1}{\Gamma(\alpha - m + 1)} \left\| \int_0^1 g(y_J(t)) dt \right\| \\ &\leq \frac{M_1}{\Gamma(\alpha - m + 1)} \int_0^1 \|g(y_J(t))\| dt \end{aligned} \tag{41}$$

Since the function  $g$  is continuous, then  $\|\mathcal{D}^m \mathcal{I}_0^\alpha \mathcal{K} y_J\|$  is bounded.

2. Let  $m \geq n$ . Motivated by the Lemma 2.21 [17], it is easy to write

$$\mathcal{D}^m \mathcal{I}_0^\alpha \mathcal{K}(y_J) = {}^C \mathcal{D}^{m-\alpha} {}^C \mathcal{D}^\alpha \mathcal{I}_0^\alpha \mathcal{K}(y_J) = {}^C \mathcal{D}^{m-\alpha} \mathcal{K}(y_J). \tag{42}$$

Taking the norm from both sides of (42) and using Lemma 2, we have

$$\begin{aligned} \|\mathcal{D}^m \mathcal{I}_0^\alpha \mathcal{K}(y_J)\| &= \|{}^C \mathcal{D}^{m-\alpha} \mathcal{K}(y_J)\| \\ &\leq \frac{1}{\Gamma(m' - m + \alpha)(m' - m + \alpha + 1)} \|\mathcal{K}(y_J)\| \quad (m' = [m - \alpha] + 1). \end{aligned} \tag{43}$$

As a result, we can bound this case according to the previous one.

Further, we can obtain

$$\|\mathcal{I}_0^\alpha (f)(x, y_J) - \mathcal{P}_J \mathcal{I}_0^\alpha (f)(x, y_J)\| \leq c_3 (r - 1)^{-m} (2^{J-1})^{-m} M_3, \tag{44}$$

and

$$\| \mathcal{I}_0^\alpha(p_1)(x, y_J) - \mathcal{P}_J \mathcal{I}_0^\alpha(p_1)(x, y_J) \| \leq c_4(r-1)^{-m} (2^{J-1})^{-m} M_4, \tag{45}$$

in which  $M_3 = \max_{\xi \in [0,1]} \{ \mathcal{D}^m \mathcal{I}_0^\alpha f(\xi, y_J(\xi)) \}$ , and  $M_4 = \max_{\xi \in [0,1]} \{ \mathcal{D}^m \mathcal{I}_0^\alpha p_1(\xi, y_J(\xi)) \}$ . Similar to the process used to calculate  $M_2$ , it can be used to approximate  $M_3$  and  $M_4$ .

If  $k$  is a continuous function and  $g$  satisfies the Lipschitz condition (3), then we can write

$$\begin{aligned} \| \mathcal{I}_0^\alpha \mathcal{K}(y) - \mathcal{I}_0^\alpha \mathcal{K}(y_J) \| &= \| \mathcal{I}_0^\alpha \left( \int_0^1 k(x, t) g(y(t)) dt - \int_0^1 k(x, t) g(y_J(t)) dt \right) \| \\ &\leq \| \mathcal{I}_0^\alpha \left( \rho \int_0^1 k(x, t) (y(t) - y_J(t)) dt \right) \| \\ &\leq \| \mathcal{I}_0^\alpha \left( \rho M_1 \int_0^1 (y(t) - y_J(t)) dt \right) \| \quad (M_1 := \max_{x,t \in [0,1]} |k(x, t)|) \\ &\leq \frac{\rho M_1}{\Gamma(\alpha)} \int_0^x (x-t)^{\alpha-1} \int_0^1 \|y - y_J\| ds dt \\ &\leq \frac{\rho M_1}{\Gamma(\alpha)} \|y - y_J\| \int_0^x (x-t)^{\alpha-1} dt \\ &\leq \frac{\rho M_1}{\alpha \Gamma(\alpha)} \|y - y_J\|. \end{aligned} \tag{46}$$

It is easy to find a bound for  $\| (\mathcal{I}_0^\alpha(f)(x, y(x)) - \mathcal{I}_0^\alpha(f)(x, y_J(x))) \|$  according to the Lemma 1, via

$$\begin{aligned} \| \mathcal{I}_0^\alpha(f)(x, y(x)) - \mathcal{I}_0^\alpha(f)(x, y_J(x)) \| &\leq \varrho \| \mathcal{I}_0^\alpha(y - y_J) \| \\ &\leq \frac{\varrho}{\Gamma(\alpha + 1)} \|y - y_J\|. \end{aligned} \tag{47}$$

Subtracting (29) from

$$y_J(x) = \mathcal{P}_J(p_1)(x) + c_1 \mathcal{P}_J(\mathcal{I}_0^\alpha(f))(x, y_J(x)) + c_2 \mathcal{P}_J(\mathcal{I}_0^\alpha(\mathcal{K}))(y_J)(x), \tag{48}$$

and taking the norm from both sides, it follows from (39), (44)–(47) that

$$\begin{aligned} \|y - y_J\| &\leq \|p_1 - \mathcal{P}_J(p_1)\| + c_1 \| \mathcal{I}_0^\alpha(f)(x, y(x)) - \mathcal{I}_0^\alpha(f)(x, y_J(x)) \| \\ &\quad + c_1 \| \mathcal{I}_0^\alpha(f)(x, y_J(x)) - c_1 \mathcal{P}_J \mathcal{I}_0^\alpha(f)(x, y_J(x)) \| \\ &\quad + c_2 \| \mathcal{I}_0^\alpha \mathcal{K}(y)(x) - \mathcal{I}_0^\alpha \mathcal{K}(y_J)(x) \| \\ &\quad + c_2 \| \mathcal{I}_0^\alpha \mathcal{K}(y_J)(x) - \mathcal{P}_J(\mathcal{I}_0^\alpha \mathcal{K}(y_J))(x) \| \\ &\leq C(r-1)^{-m} (2^{J-1})^{-m} + \eta \|y - y_J\| \end{aligned} \tag{49}$$

in which  $C = c_4 M_4 + c_1 c_3 M_3 + c_2 c_0 M_2$  and  $\eta = c_1 \frac{\varrho}{\Gamma(\alpha+1)} + c_2 \frac{\rho M_1}{\alpha \Gamma(\alpha)}$ . If  $\eta < 1$ , then we can bound the error as follows.

$$\|y(x) - y_J(x)\| \leq \frac{C}{1-\eta} (r-1)^{-m} (2^{J-1})^{-m}. \tag{50}$$

□

#### 4. Numerical Experiments

All numerical computations were carried out simultaneously using Maple and Matlab software.

**Example 1.** Consider the following equation [23] as the first example.

$${}^C\mathcal{D}_0^{5/6}u(x) + \int_0^1 xe^t(u(t))^2 dt = \frac{3}{\Gamma(1/6)} \left( 2\sqrt[6]{x} - \frac{432}{91}\sqrt[6]{x^{13}} \right) - x(248e - 674),$$

with initial condition  $u(0) = 0$ . The exact solution is reported in [23] as  $u(x) = x - x^3$ .

Table 1 gives a comparison between the proposed method and Alpert’s multi-wavelets method. It can be seen that our method offers better accuracy. The  $L_\infty$ -error is reported for different values of  $r$  ( $N = r2^J$ ) and  $x$  in Table 2. To show the effect of the parameters  $\mu$  and  $r$  in the  $L^2$ -error, we plot the Figure 1.

**Table 1.** The comparison between Alpert’s multiwavelets method and the proposed method taking  $\mu = 5/6$  and Chebyshev nodes for Example 1.

	Proposed Method			Alpert’s Multiwavelets Method [23]
	$N = 4$	$N = 5$	$N = 7$	$N = 96$
$L^2$ -error	$1.78 \times 10^{-3}$	$4.08 \times 10^{-4}$	$1.72 \times 10^{-4}$	$1.43 \times 10^{-3}$

**Table 2.** The  $L_\infty$ -error taking  $\mu = 5/6$  for Example 1.

		$x = 0.1$	$x = 0.3$	$x = 0.5$	$x = 0.7$	$x = 0.9$
Chebyshev nodes	$N = 5$	$6.62 \times 10^{-4}$	$3.41 \times 10^{-4}$	$2.17 \times 10^{-4}$	$1.98 \times 10^{-6}$	$1.89 \times 10^{-4}$
	$N = 7$	$1.65 \times 10^{-5}$	$2.09 \times 10^{-6}$	$9.63 \times 10^{-6}$	$2.77 \times 10^{-5}$	$6.68 \times 10^{-5}$
Legendre nodes	$N = 5$	$2.84 \times 10^{-4}$	$6.80 \times 10^{-5}$	$2.19 \times 10^{-4}$	$2.70 \times 10^{-4}$	$4.69 \times 10^{-5}$
	$N = 7$	$2.95 \times 10^{-4}$	$1.07 \times 10^{-4}$	$9.61 \times 10^{-6}$	$8.85 \times 10^{-5}$	$1.48 \times 10^{-4}$

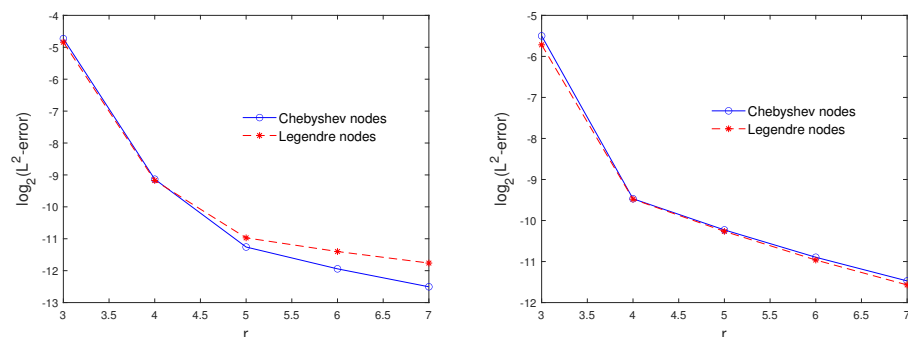


**Figure 1.** The  $L^2$ -errors for  $\mu = 1$  (right) and  $\mu = 5/6$  (left) at the Chebyshev and Legendre nodes for Example 1.

**Example 2.** Consider the nonlinear FFIDEs [23]

$${}^C\mathcal{D}_0^{1/2}u(x) + \int_0^1 xt(u(t))^4 dt = \frac{1}{\Gamma(1/2)} \left( 8/3x^{3/2} - 2x^{1/2} \right) - \frac{x}{1260}, \quad x \in [0, 1]$$

subject to the initial condition  $u(0) = 0$ . The exact solution is  $u(x) = x^2 - x$  [23].

To show the effect of the parameter  $r$  in the  $L^2$ -error, we plot the Figure 2. A comparison between the proposed method and Alpert’s multi-wavelets method is reported in Table 3. The  $L_\infty$ -error is reported for different values of  $r$  ( $N = r2^J$ ) and  $x$  in Table 4. With fewer bases, the proposed method shows better accuracy than the Alpert’s multi-wavelets method. Figure 3 illustrates the exact and approximate solutions at the Chebyshev nodes with different numbers of bases.

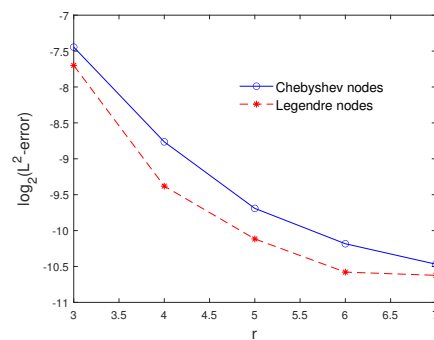


Figure 2. The  $L^2$ -errors for  $\mu = 1$  at the Chebyshev and Legendre nodes for Example 2.

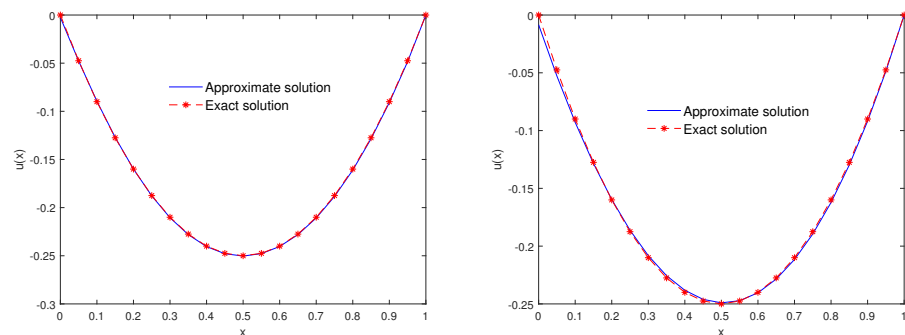


Figure 3. Plot of the exact and approximate solutions taking  $r = 7$  (left) and  $r = 5$  (right) at Chebyshev nodes for Example 2.

Table 3. The  $L_\infty$ -error taking  $\mu = 1$  for Example 2.

		$x = 0.1$	$x = 0.3$	$x = 0.5$	$x = 0.7$	$x = 0.9$
Chebyshev nodes	$N = 5$	$4.39 \times 10^{-4}$	$8.10 \times 10^{-4}$	$9.42 \times 10^{-4}$	$1.10 \times 10^{-3}$	$4.81 \times 10^{-4}$
	$N = 7$	$5.03 \times 10^{-4}$	$4.94 \times 10^{-4}$	$2.88 \times 10^{-4}$	$7.34 \times 10^{-4}$	$3.57 \times 10^{-4}$
Legendre nodes	$N = 5$	$8.95 \times 10^{-5}$	$1.30 \times 10^{-4}$	$9.42 \times 10^{-4}$	$3.22 \times 10^{-4}$	$8.72 \times 10^{-4}$
	$N = 7$	$2.56 \times 10^{-5}$	$8.63 \times 10^{-5}$	$2.88 \times 10^{-4}$	$9.01 \times 10^{-5}$	$7.25 \times 10^{-4}$

Table 4. Comparison between Alpert’s multiwavelets method and the proposed method taking  $\mu = 1$  and Legendre nodes for Example 2.

	Proposed Method			Alpert’s Multiwavelets Method [23]
	$N = 5$	$N = 6$	$N = 7$	$N = 96$
$L^2$ -error	$9.01 \times 10^{-4}$	$6.54 \times 10^{-4}$	$6.34 \times 10^{-4}$	$1.17 \times 10^{-4}$

Example 3. Let us dedicate the third example to the nonlinear equation

$${}^C D_0^\beta u(x) + 3x^2 u^4(x) - \int_0^1 x^2(t+1)u^2(t)dt = \frac{18x^4\Gamma(\frac{3}{2}-\beta) - 5x^2\Gamma(\frac{3}{2}-\beta) + 3\sqrt{\pi}x^{1/2-\beta}}{6\Gamma(\frac{3}{2}-\beta)}$$

where  $0 < \beta \leq 1$  and the exact solution is  $u(x) = \sqrt{x}$ .

Figure 4 is plotted to verify the effect of the parameter  $r$ . The  $L_\infty$ -error is reported for different values of  $r$  ( $N = r2^j$ ) and  $x$  in Table 5. Figure 5 illustrates the exact and approximate solutions at the Chebyshev and Legendre nodes.

**Table 5.** The  $L_\infty$ -error taking  $\beta = 1/3$  and  $\mu = 1/3$  for Example 3.

		$x = 0.1$	$x = 0.3$	$x = 0.5$	$x = 0.7$	$x = 0.9$
Chebyshev nodes	$N = 5$	$8.60 \times 10^{-4}$	$1.59 \times 10^{-4}$	$1.46 \times 10^{-4}$	$6.49 \times 10^{-5}$	$3.36 \times 10^{-5}$
	$N = 8$	$5.58 \times 10^{-5}$	$1.05 \times 10^{-5}$	$1.67 \times 10^{-5}$	$1.66 \times 10^{-5}$	$1.36 \times 10^{-5}$
Legendre nodes	$N = 5$	$6.62 \times 10^{-4}$	$1.16 \times 10^{-4}$	$1.48 \times 10^{-4}$	$5.55 \times 10^{-5}$	$3.25 \times 10^{-5}$
	$N = 8$	$2.28 \times 10^{-5}$	$8.03 \times 10^{-6}$	$1.71 \times 10^{-5}$	$1.53 \times 10^{-5}$	$1.44 \times 10^{-5}$

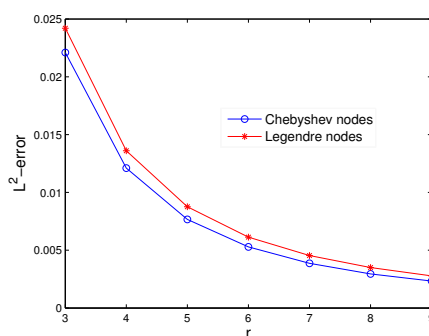


**Figure 4.** The  $L^2$ -errors for  $\beta = 1/2$  and  $\mu = 1$  at the Chebyshev and Legendre nodes for Example 3.

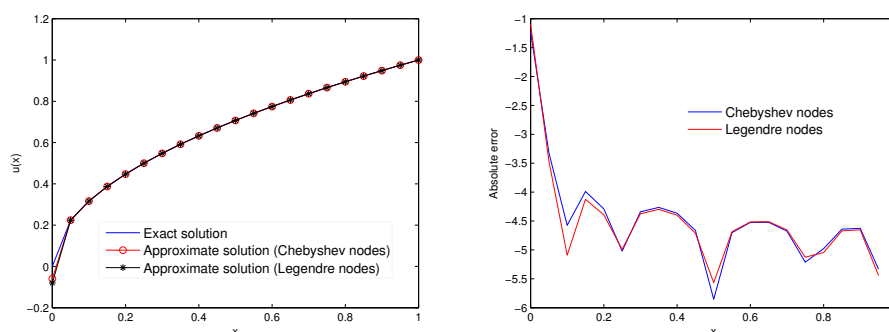


**Figure 5.** Plot of the exact and approximate solutions (left) and absolute error (right) taking  $r = 7$  and  $\beta = \mu = 1/3$  at Chebyshev and Legendre nodes for Example 3.

### 5. Conclusions

In the present paper, the wavelet collocation method has been used to solve the fractional Fredholm integral differential equations. After converting this problem to an equivalent linear or nonlinear weakly singular Volterra–Fredholm integral equation, we apply the wavelet collocation method based on ML wavelets to solve this integral equation. To do this, the fractional integral operator based on ML wavelets is represented as a matrix and then the collocation method is used to reduce the problem to a linear or nonlinear system of algebraic equations. An a posteriori error estimate for the method is investigated. To demonstrate the ability and accuracy of the method, some numerical examples are presented. The results are compared with other existing methods and demonstrate that this method offers better results.

**Author Contributions:** Conceptualization, H.B.J. and I.D.; methodology, H.B.J.; software, H.B.J. and I.D.; validation, H.B.J. and I.D.; formal analysis, H.B.J. and I.D.; investigation, H.B.J. and I.D.; writing—original draft preparation, H.B.J. and I.D.; writing—review and editing, H.B.J. and I.D.; visualization, H.B.J. and I.D.; supervision, H.B.J.; project administration, H.B.J. and I.D.; funding acquisition, H.B.J. All authors have read and agreed to the published version of the manuscript.

**Funding:** This work is supported by the Researchers Supporting Project Number (RSP-2021/210), King Saud University, Riyadh, Saudi Arabia.

**Institutional Review Board Statement:** Not applicable.

**Informed Consent Statement:** Not applicable.

**Data Availability Statement:** The data presented in this study is available on request from the corresponding author.

**Conflicts of Interest:** The writers state that they have no known personal relationships or competing financial interests that could have appeared to affect the work reported in this work.

### Abbreviations

The following abbreviations are used in this manuscript:

FFIDEs	fractional Fredholm integro-differential equations
ML	Müntz–Legendre
RL	Riemann–Liouville

### References

- Aminikhah, H. A new analytical method for solving systems of linear integro-differential equations. *J. King Saud Univ. Sci.* **2011**, *23*, 349–353. [\[CrossRef\]](#)
- Angstmann, C.N.; Henry, B.I.; McGann, A.V. A fractional order recovery SIR model from a stochastic process. *Bull. Math. Biol.* **2016**, *78*, 468–499. [\[CrossRef\]](#) [\[PubMed\]](#)
- Eslahchi, M.R.; Dehghan, M.; Parvizi, M. Application of the collocation method for solving nonlinear fractional integro-differential equations. *J. Comput. Appl. Math.* **2014**, *257*, 105–128. [\[CrossRef\]](#)
- Rawashdeh, E.A. Numerical solution of fractional integro-differential equations by collocation method. *Appl. Math. Comput.* **2006**, *176*, 1–6. [\[CrossRef\]](#)
- Momani, S.; Noor, M.A. Numerical methods for fourth order fractional integro-differential equations. *Appl. Math. Comput.* **2006**, *182*, 754–760. [\[CrossRef\]](#)
- Momani, S.; Qaralleh, A. An Efficient Method for Solving Systems of Fractional Integro-Differential Equations. *Comput. Math. Appl.* **2006**, *52*, 459–470. [\[CrossRef\]](#)
- Zhu, L.; Fan, Q. Solving fractional nonlinear Fredholm integro-differential equations by the second kind Chebyshev wavelet. *Commun. Nonlinear Sci. Numer. Simul.* **2012**, *17*, 2333–2341. [\[CrossRef\]](#)
- Arikoglu, A.; Ozkol, I. Solution of fractional integro-differential equations by using fractional differential transform method. *Chaos Solitons Fractals* **2009**, *40*, 521–529. [\[CrossRef\]](#)
- Saeedi, H.; Mohseni Moghadam, M.; Mollahasani, N.; Chuev, G.N. A CAS wavelet method for solving nonlinear Fredholm integro-differential equations of fractional order. *Commun. Nonl. Sci. Numer. Simul.* **2011**, *16*, 1154–1163. [\[CrossRef\]](#)
- Shahmorad, S.; Ostadzad, M.H.; Baleanu, D. A Tau-like numerical method for solving fractional delay integro-differential equations. *Appl. Numer. Math.* **2019**, *151*, 322–336. [\[CrossRef\]](#)
- Baleanu, D.; Rezapour, S.; Saberpour, Z. On fractional integro-differential inclusions via the extended fractional Caputo-Fabrizio derivation. *Bound. Value Probl.* **2019**, *2019*, 79. [\[CrossRef\]](#)
- Baleanu, D.; Mousalou, A.; Rezapour, S. A new method for investigating approximate solutions of some fractional integro-differential equations involving the Caputo-Fabrizio derivative. *Adv. Differ. Equ.* **2017**, *2017*, 51. [\[CrossRef\]](#)
- Rahimkhani, P.; Ordokhani, Y.; Babolian, E. Müntz-Legendre wavelet operational matrix of fractional-order integration and its applications for solving the fractional pantograph differential equations. *Numer. Algorithms* **2018**, *77*, 1283–1305. [\[CrossRef\]](#)
- Rahimkhani, P.; Ordokhani, Y. Numerical solution a class of 2D fractional optimal control problems by using 2D Müntz-Legendre wavelets. *Optim. Control. Appl. Methods* **2018**, *39*, 1916–1934. [\[CrossRef\]](#)
- Mokhtary, P.; Ghoreishi, F.; Srivastava, H.M. The Müntz-Legendre tau method for fractional differential equations. *Appl. Math. Model.* **2016**, *40*, 671–684. [\[CrossRef\]](#)
- Bin Jebreen, H.; Tchier, F. A New Scheme for Solving Multiorder Fractional Differential Equations Based on Müntz–Legendre Wavelets. *Complexity* **2021**, *2021*, 9915551. [\[CrossRef\]](#)
- Kilbas, A.; Srivastava, H.M.; Trujillo, J.J. *Theory and Applications of Fractional Differential Equations*; Elsevier: Amsterdam, The Netherlands, 2006; Volume 204.
- Mallat, S.G. *A Wavelet Tour of Signal Processing*; Academic Press: Cambridge, MA, USA, 1999.
- Almira, J.M. Müntz type theorems I. *Surv. Approx. Theory* **2007**, *3*, 152–194.
- Müntz, C.H. *Über den Approximationssatz von Weierstrass*; Springer: Berlin/Heidelberg, Germany, 1914; pp. 303–312.
- Shen, J.; Wang, Y. Müntz-Galerkin methods and applicationa to mixed dirichlet-neumann boundary value problems. *SIAM J. Sci. Comput.* **2016**, *38*, 2357–2381. [\[CrossRef\]](#)
- Borwein, P.; Erdélyi, T.; Zhang, J. Müntz systems and orthogonal Müntz–Legendre polynomials. *Trans. Am. Math. Soc.* **1994**, *342*, 523–542.
- Paseban-Hag, S.; Osgooei, E.; Ashpazzadeh, E. Alpert wavelet system for solving fractional nonlinear Fredholm integro-differential equations. *Comput. Methods Differ. Equ.* **2021**, *9*, 762–773.